Applications of Simultaneous Tracking with Optical Sensors

Zach Slatton[(1)], Albert Butkus[(2)], Robert Bruck[(3)]

[(1)]HQ AFSPC/A3/6Z, zachary.slatton@us.af.mil, CO, USA

[(2)]SENSOR, CO, USA

[(3)]20 SPCS/Det 3, HI, USA

ABSTRACT

Due to the new additions to the United States Space Surveillance Network (SSN), it is necessary to reevaluate the usefulness of triangulated range and to operationalize new concepts that take advantage of stereoscopic tracking. This paper presents new tasking and search concepts for ground-based optical sensors. These concepts utilize synchronized, stereoscopic tracking of resident space objects to allow for faster processing of maneuvers and uncorrelated tracks (UCTs). Due to these concepts, the amount of ground-based simultaneous tracks from the SSN have been increased by a factor of ten to twenty which greatly increases the accuracy of short arc fits in the geosynchronous regime. The triangulation algorithm presented previously has also been improved upon to increase the accuracy of the derived range by correcting for light-time as well as smoothing the tracks to perfectly synchronize the observations.

1 BACKGROUND

The geosynchronous (GEO) belt is a challenging regime to maintain, primarily because of the decrease in detectability due to the range of the objects residing in this orbit. For radars, the detectability is inversely proportional to R^4, where R is the slant range from the sensor to the satellite. For optical sensors, the detectability is inversely proportional to R^2. For this reason, primarily optical sensors track most of the debris in the GEO region. However, optical sensors cannot observe range. Without range, the time needed to perform accurate initial orbit determination and time to process maneuvers increases by a factor of four.

In 2013-2014, two of the US Space Surveillance System's (SSN) ground-based optical (GBO) sites and the Joint Space Operations Center (JSpOC) performed an experiment where the sites tracked resident space objects (RSOs) simultaneously. JSpOC analysts were able to derive a range through triangulation and increase the accuracy of the objects' two line element sets (TLEs). These TLEs were returned to the site for further tracking. The accuracy increase was more apparent for objects with minimal data, such as UCTs, newly launched objects, and objects that had just maneuvered. These are examples of the short arc problem. The range was determined to be accurate enough to be used in a Simplified General Perturbations 4 (SGP4) Differential Correction (DC), but not a Special Perturbations (SP) DC.

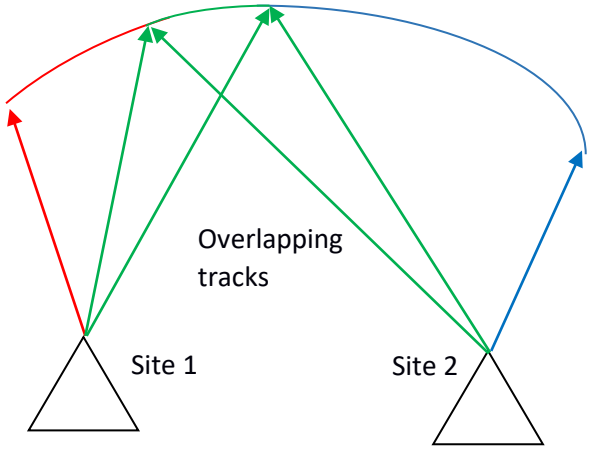

Fig. 1. Simultaneous Tracking to Derive Range

2 SSN ADDITIONS

Since the previous work [5], the SSN has acquired an abundance of space-based optical (SBO) data. With these new additions, the SSN serendipitously produces hundreds overlapping tracks a day from various optical sources. The vast majority of these include SBO observations. Future additions to the SSN will include additional GBO and SBO sensors as well as commercial network augmentation, which will increase the number of overlapping tracks per day. With these new capabilities, there needed to be a reevaluation of the effectiveness of the triangulated range.

3 ALGORITHM IMPROVEMENTS

A limitation of the triangulation algorithm is that the observations have to be precisely simultaneous which is extremely difficult to coordinate when the sites are on systems that do not communicate with each other. The previous work [5] adopted a simple interpolation to synchronize the observations before accomplishing the triangulation. This has been found to be less accurate than desired for an SP DC. The algorithm now utilizes a variable order, least-squares polynomial regression fit on the right ascension and declination to smooth the data. The new polynomial is then used to generate synchronized observations so that the range can be triangulated. After the range is found, another fit is done over the triangulated range of the track to smooth the output. Using the derived range, a light-time correction can then be applied iteratively. This process usually converges in around three iterations. These new improvements can increase the accuracy of the range by up to a factor of two for GBO-only triangulations. Unfortunately, there will always be a few hundred meters of error due to the noise of the angle measurements. Another improvement over the previous method is that smoothing the angles provides right ascension-rates and declination-rates, while smoothing the range provides range-rates. This gives six observables as opposed to the two normally provided by optical sites.

For SBO sensors, the position of the sensor needs to be accounted for as well. This adds three more variables that need to be smoothed and interpolated (X, Y, Z components of position). Due to the uncertainty in the sensor position, the triangulated ranges will be less accurate than a GBO-only triangulation, sometimes by kilometers. Even though the range is worse, it will still be valuable in short arc solutions if weighted properly.

There were cases where the triangulated range residuals were found to be off by several kilometers. This sometimes happens when any of the stereoscopic angles are small (See Appendix A for calculation). The stereoscopic angles are defined as the angles of the triangle made up of the two intersecting lines of sight as well as the vector from one site to the other. Cases where any of the stereoscopic angles are less than a certain minimum are rejected in this work. Five degrees has been observed to be a good minimum.

Figure 2 displays the process of smoothing the observations and triangulating the range. Figure 3 shows the residuals of the range (in meters) derived using the original method. Figure 4 shows the residuals after smoothing the angles and range as well as correcting for light-time. With the new corrections, the accuracy of the residuals is greatly increased.

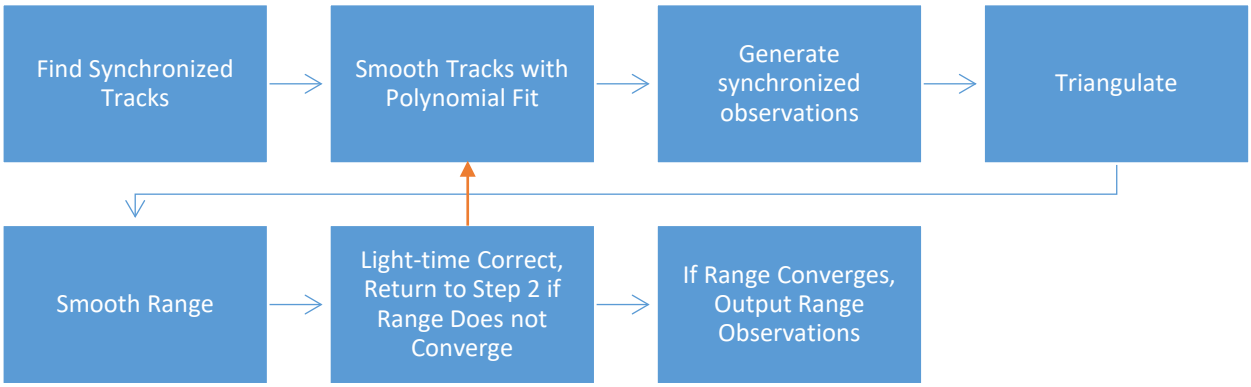

Fig. 2. Triangulation Process

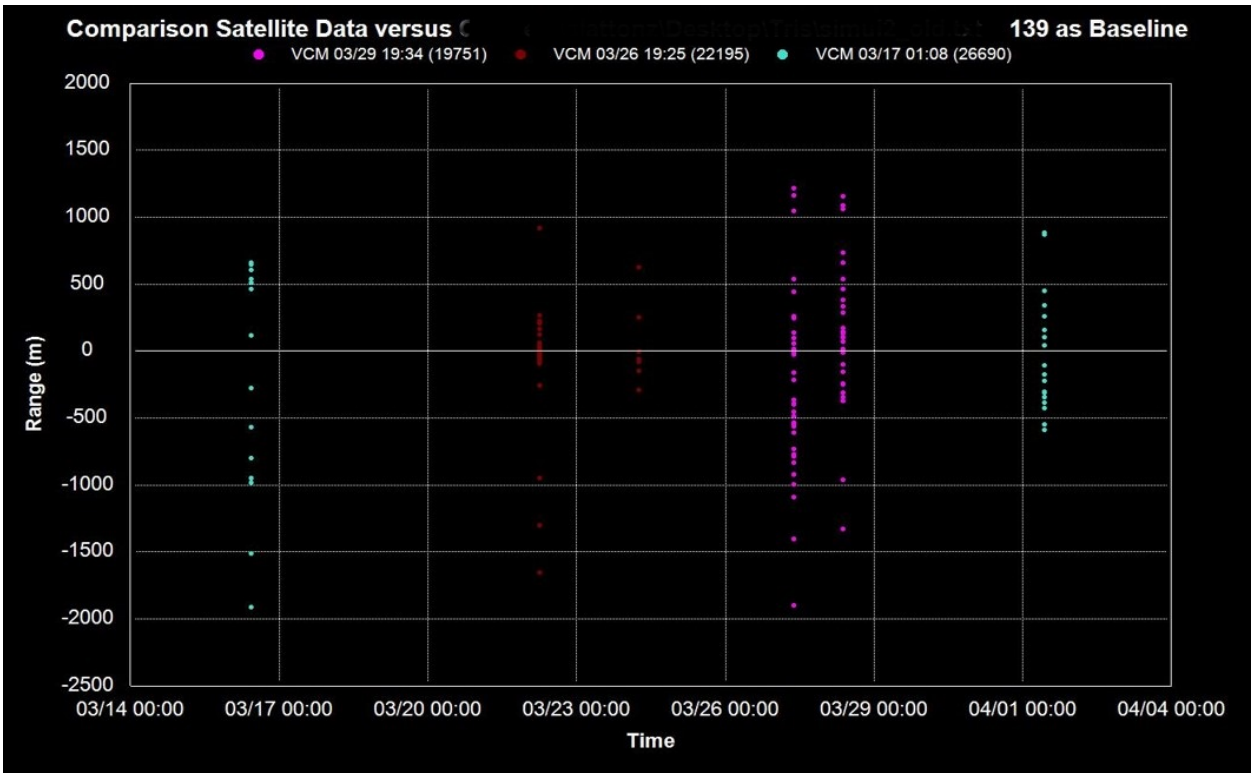

Fig. 3. Triangulated Range Residuals (Original Method)

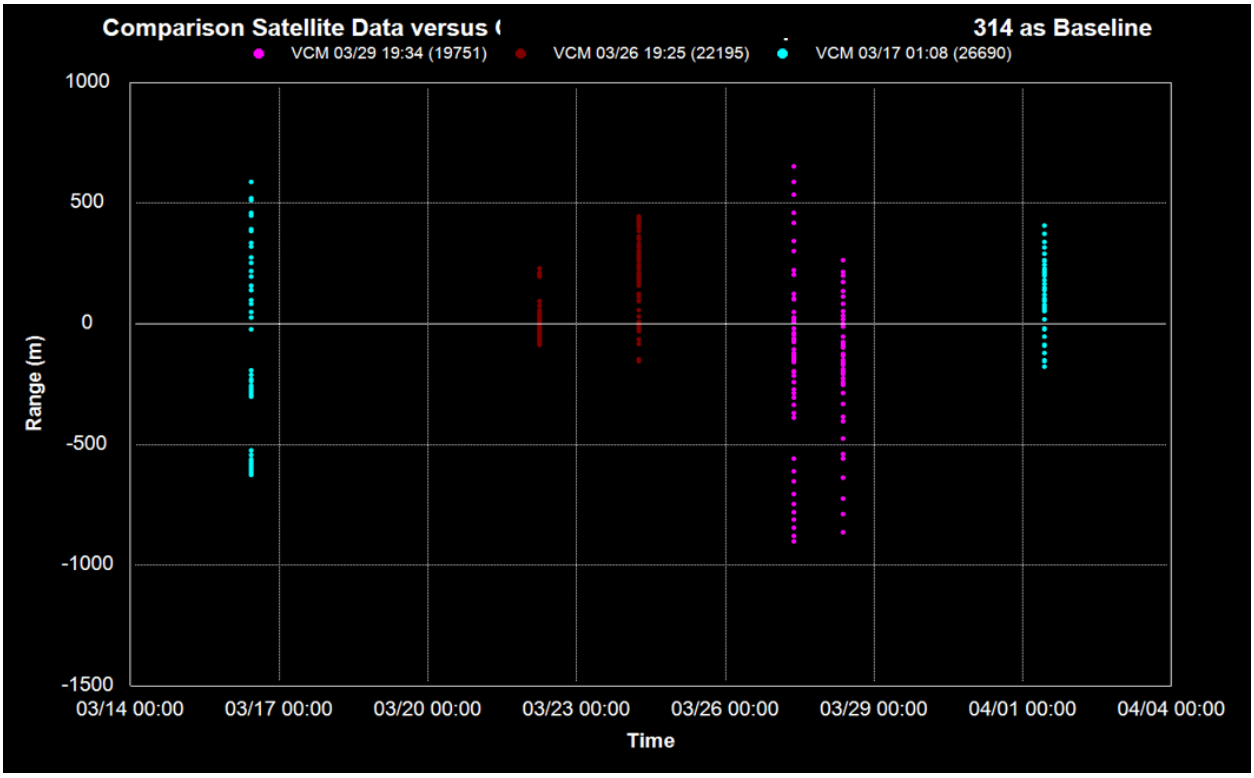

Fig. 4. Triangulated Range Residuals (New Method)

4 PROPAGATION METRIC ANALYSIS

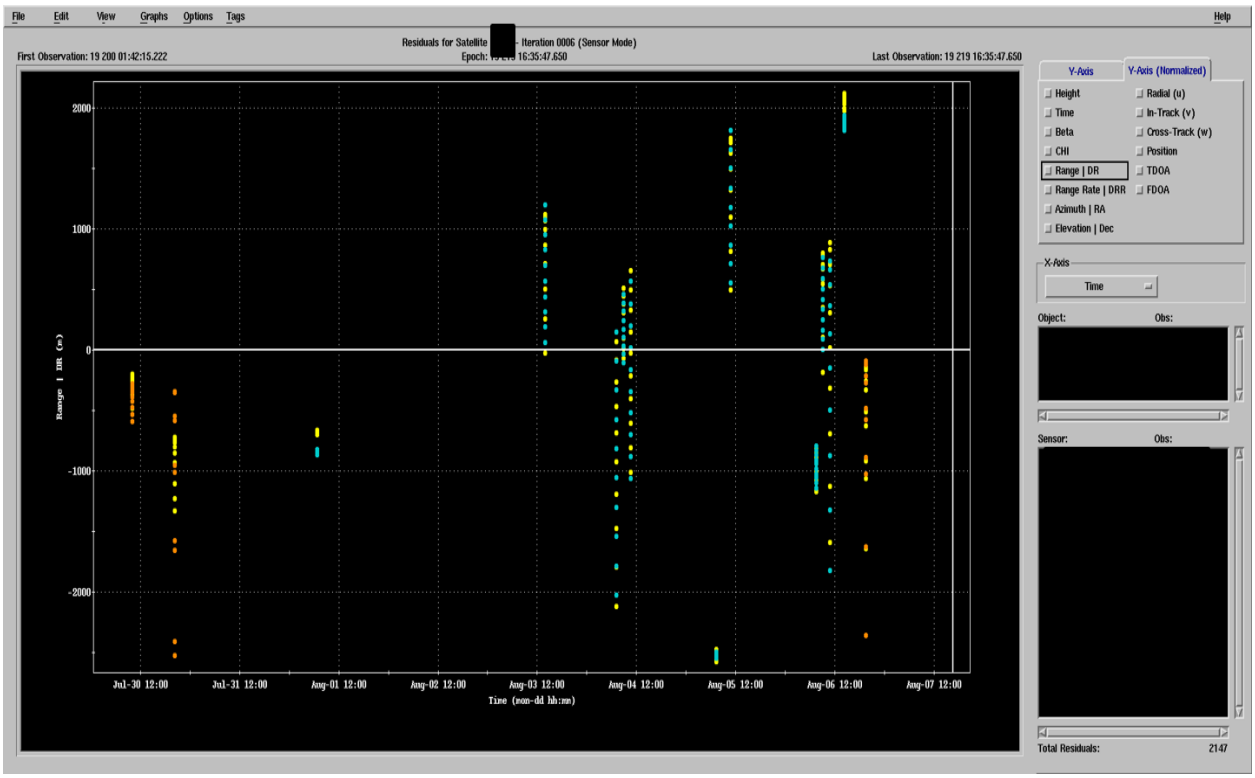

Fig. 5. GBO and SBO Triangulated Range Residuals

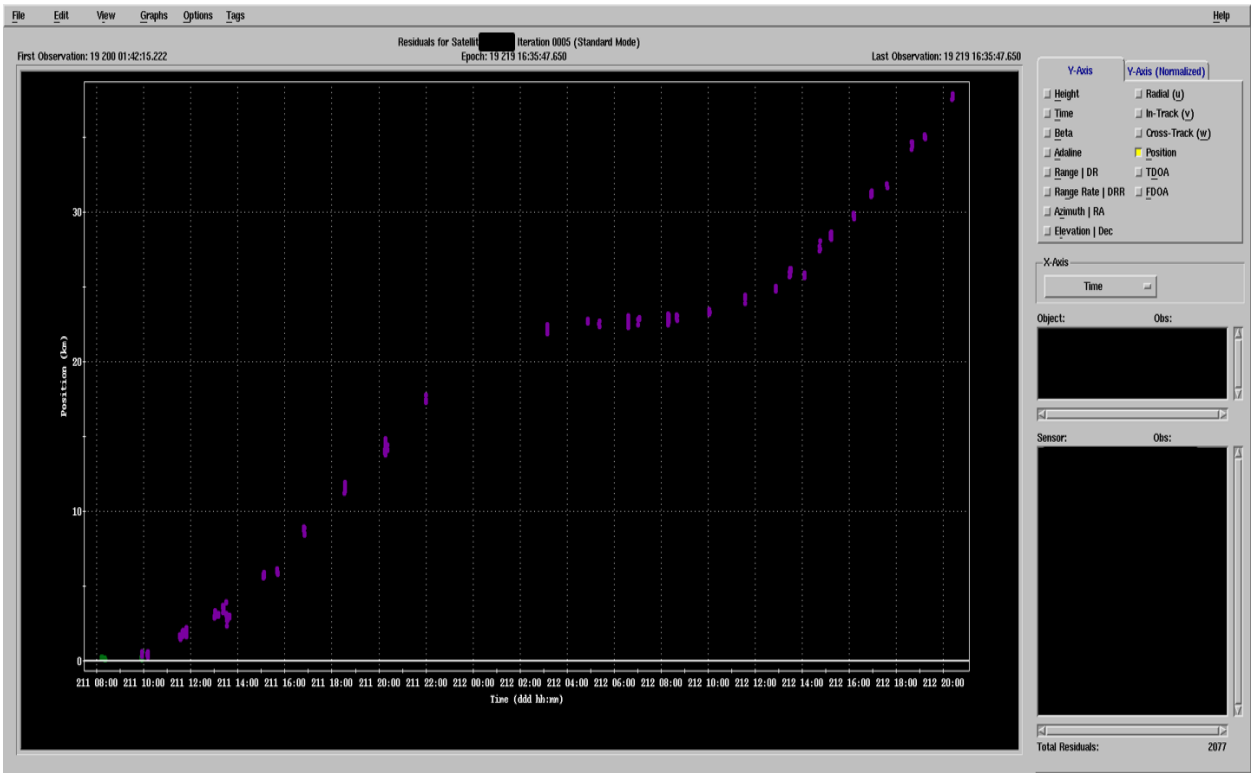

Fig. 6. Post Maneuver Position Residuals with Angles Only

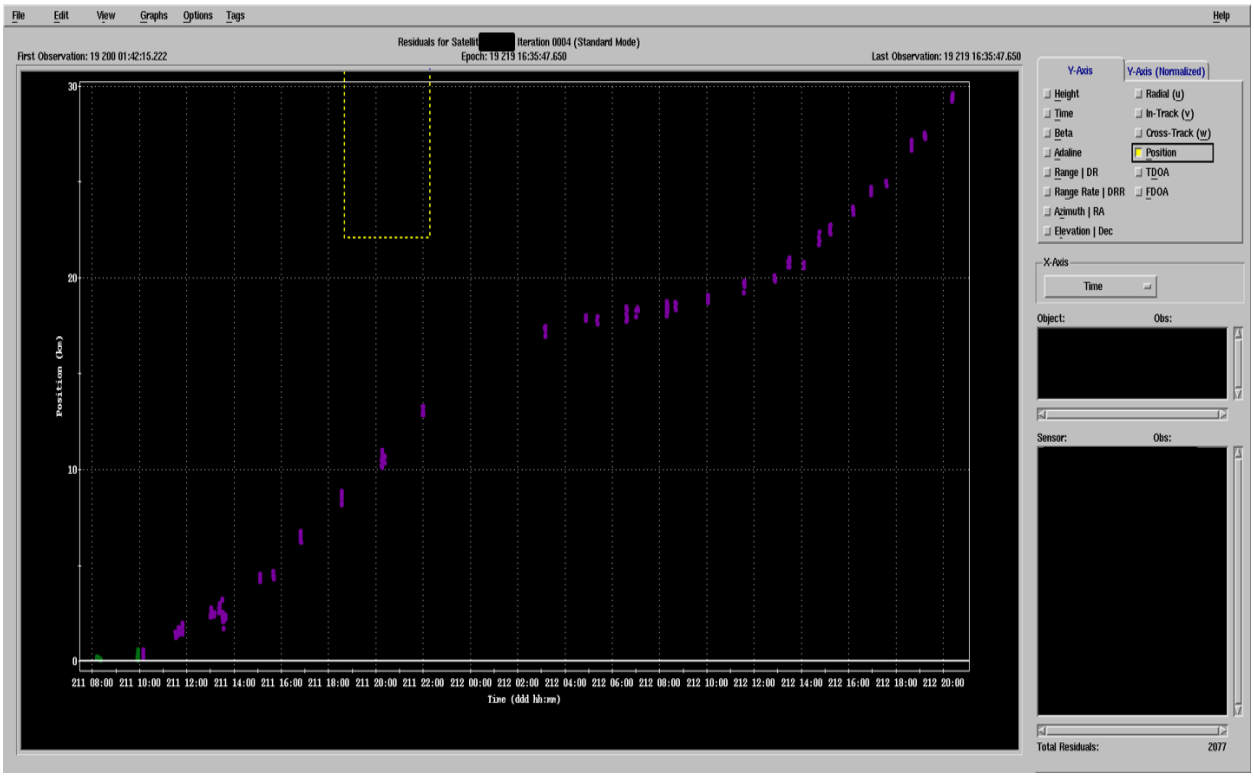

Fig. 7. Post Maneuver Position Residuals with Triangulated Range

Figure 5 shows triangulated range residuals when near-earth, space-based optical sensors are used to track a geosynchronous object. The standard deviation of the ranges is around 1100 meters. Figures 6 and 7 show position residuals for a geosynchronous payload that maneuvered and was simultaneously tracked shortly after by two SBOs. The satellite was processed with a weighted differential correction with and without using a triangulated range track, and the residuals of position after the differential correction were compared. The following night's residuals showed a 23% increase in accuracy when including the triangulated range track.

5 PROPAGATION COVARIANCE ANALYSIS

A short covariance analysis was accomplished using the post-maneuver geosynchronous test case in Fig. 5-7. Table 1 shows the Radial, In-track, and Cross Track (U, V, and W respectively) standard deviations (σ) at epoch. The short arc case was examined as well as the full solution with eight days of observations. When triangulated ranges are included in the differential correction, there was a 3-4% reduction in the U σ, V σ, and W σ for the full solution. There was a 4-5% reduction in the V σ and W σ the short arc solution and a 15% reduction in the U σ. This is to be expected since a radial measurement cannot be accurately derived for most sensors without accurate range. For optical sensors, the state vector is used to derive synthetic range to calculate the radial measurements of the tracked object. However, this is usually inaccurate for a short arc solution.

Table 1. Covariance Reduction of Post Maneuver GEO at Epoch

	U σ	V σ	W σ
Reduction of full solution	3.59%	3.30%	4.55%
Reduction of short arc solution	15.27%	4.53%	5.09%

Having a smaller covariance is only meaningful if it is realistic. Covariance realism analysis is accomplished by comparing the propagated position, X_{prop}, and covariance P_{prop}, to a truth source, X_{truth}, and its covariance, P_{truth}, then calculating the Mahalanobis distance, M [3].

$$M = (X_{truth} - X_{prop})^T * (P_{truth} + P_{prop})^{-1} * (X_{truth} - X_{prop}) \quad (1)$$

It follows that M is chi-square distributed with n degrees of freedom, where n is the dimension of the state vector X. In this analysis, $n = 3$. A 99% one-sided confidence interval for M is [0, 11.345]. Therefore, if M falls outside this interval, we declare a breakdown in covariance realism.

The Mahalanobis distance of the short arc solution using triangulated range was compared to the short arc, angles only solution by using the full solution as truth. The full solution included eight days of dense angles only data after the maneuver. The analysis period was from the time of the maneuver to the epoch of the full solution. As can be seen in Fig. 8, the Mahalanobis distance degrades significantly at a certain part of the orbit. This corresponds to the sections of the orbit that had no tracking data. This is where covariance realism breaks down. However, the solution that includes the triangulated range almost perfectly matches the angles only solution at every time step, meaning covariance realism was not degraded by introducing triangulated range to the solution.

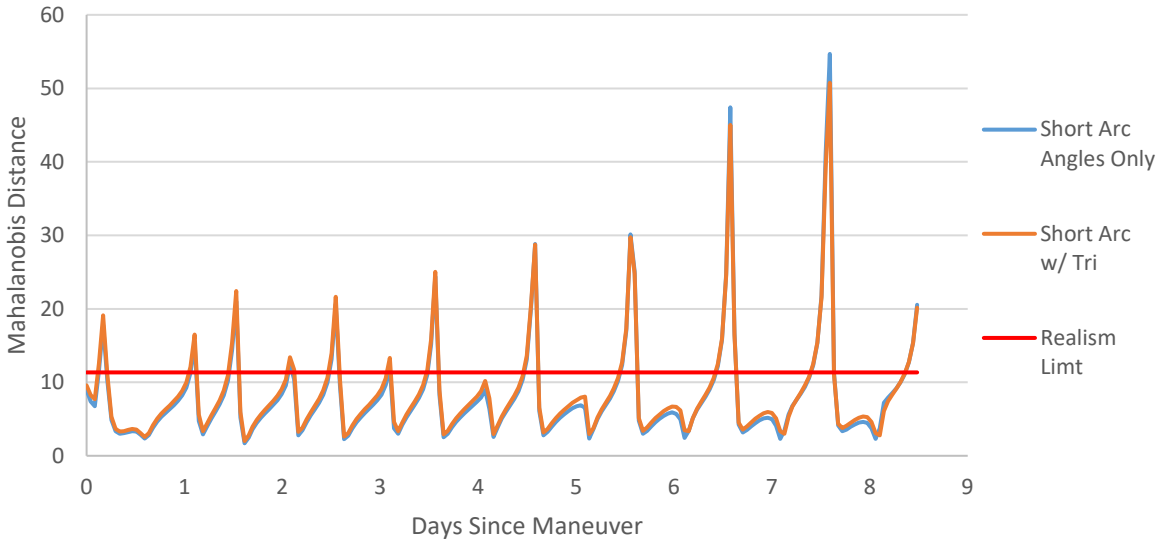

Fig. 8. Mahalanobis Distance of Short Arc Solution with and without Triangulated Range

6 SIMULTANEOUS TASKING CONCEPTS

The SSN's GBO systems are very agile. Tasking can be done near-real time, which guarantees simultaneous tracking if both sites are available and the desired object is detectable. If the first site discovers an object has maneuvered, it can call the second site to track the object simultaneously if the object is in coverage at both sites. Alternatively, if the command and control (C2) center finds a maneuvered object, it can task the sites for simultaneous tracks. This will decrease the time needed to process the maneuver and send an updated TLE to the site.

7 UNCORRELATED TRACK (UCT) HANDOFF CONCEPT

When the SSN's GBO sites track a UCT, they will attempt to follow up throughout the tracking period. These sites also have the capability to handoff TLEs. This is accomplished by doing a differential correction on all of the tracks of a UCT and passing the resulting TLE to another site. This has been done successfully numerous times to great success. The sites have also simultaneously tracked UCTs after handoff. One of the resulting TLEs incorporating triangulated range was able to associate with less than 20 kilometers of error for up to three nights afterwards. Without the range, the TLE had around 170 kilometers of error three nights later.

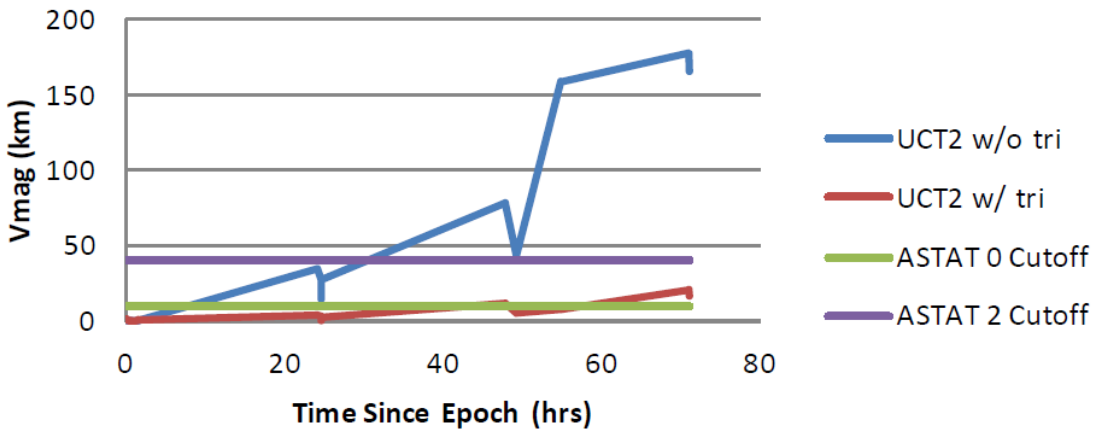

Fig. 9. Error Growth of UCT with Triangulated Range [5]

8 GROUND-BASED OPTICAL SEARCH CONCEPT

A new idea is proposed where two GBO sites with overlapping coverage perform a simultaneous geosynchronous search of the overlapping longitudes. The sites begin tracking at the same longitude and finish at a different longitude simultaneously tracking every object in the search pattern. This is an uncued method of collecting simultaneous tracks. The benefits of this are that an object does not have to be tasked or in the catalog to be tracked. Some precautions have to be taken to ensure the search remains in sync, however. The sites will search faster near the horizon since it takes fewer fields of view. For this reason, the search is started ten degrees of longitude off the horizon. The sites can also get out of sync due to weather or other reasons, so the search is broken into segments to ensure the sites can maintain synchronicity.

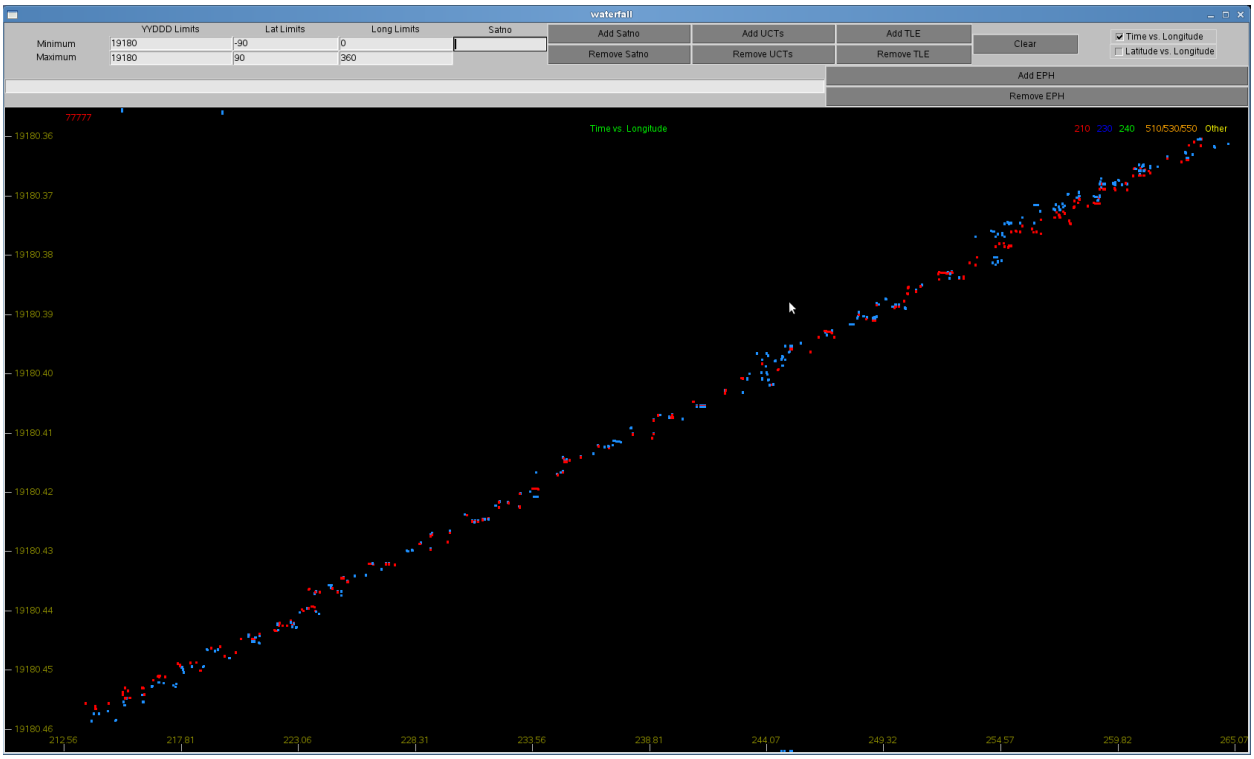

Fig. 10. Time (reversed) vs. Longitude of Synchronized Search

Figure 10 shows a successful synchronized search conducted on 2019 day 180. The sensors start around 265 degrees of longitude and end around 214 degrees of longitude. The tracks of site one (red) and site two (blue) coincide when the objects are tracked simultaneously. During the searches, the number of GBO-only simultaneous tracks per night increased by a factor of ten to twenty.

9 CONCLUSION

The improvements in the triangulation algorithm have greatly increased the derived range accuracy from the experiments done in 2013-2015. With the increase in sensors in the SSN, new search methods, and new tasking methods, there is a vast increase in the number of simultaneous tracks. The range derived from these tracks will decrease processing time of maneuvered objects, newly launched objects, and UCTs while increasing accuracy of the deep space regime where range measurements are sparse.

10 REFERENCES

1. D. A. Cicci, “Implementation of Ridge-Type Estimation Methods Using Orthogonal Transformations,” *IEEE Transactions on Automatic Control,* vol. 37, no. 11, pp. 1834-1837, Nov 1992.

2. E. W. Weisstein, "Least Squares Fitting--Polynomial." From *MathWorld*--A Wolfram Web Resource. http://mathworld.wolfram.com/LeastSquaresFittingPolynomial.html

3. J. T. Horwood, J. M. Aristoff, N. Singh, A. B. Poore, and M. D. Hejduk, “Beyond covariance realism: a new metric for uncertainty realism,” in Proceedings of the SPIE, Signal and Data Processing of Small Targets, Vol. 9092, Baltimore, MD, May 2014

4. P. Schumacher, Personal Communication, September 2014.

5. Z. Slatton, "A Short Evaluation of Triangulated Range from Multiple Angles-Only Sites" in Proceedings of the 2014 AMOS Technical Conference, Wailea, Maui, HI, 2014.

Appendix A: Triangulation Algorithm [5]

For the position of a satellite:

$$\rho * \hat{\rho} + \vec{R} = \vec{r} \tag{2}$$

Where ρ is the range, $\hat{\rho}$ is the pointing vector, $\vec{R}$ is the sensor position in the earth-centered inertial (ECI) coordinate frame, and $\vec{r}$ is the satellite position, also in the ECI coordinate frame.

$$\hat{\rho} = \begin{bmatrix} \cos(\delta_t) * \cos(\alpha_t) \\ \cos(\delta_t) * \sin(\alpha_t) \\ \sin(\delta_t) \end{bmatrix} \tag{3}$$

Where δ_t is the topocentric declination and α_t is the topocentric right ascension.

If two sensors track the satellite at the same time, the equation can be written as:

$$\rho_1 * \hat{\rho}_1 + \vec{R}_1 = \rho_2 * \hat{\rho}_2 + \vec{R}_2 \tag{4}$$

The range can then be solved by the least squares solution of the equation:

$$\begin{bmatrix} \hat{\rho}_1 & -\hat{\rho}_2 \end{bmatrix} * \begin{bmatrix} \rho_1 \\ \rho_2 \end{bmatrix} = \vec{R}_2 - \vec{R}_1 \tag{5}$$

This least squares equation is solved with a modified Householder orthogonal decomposition [1]. The advantage of this algorithm is that the matrix does not have to be squared to be inverted allowing the numerical precision to be better maintained.

It is important to note that when any of the stereoscopic angles, θ, are small, the results will sometimes be less accurate. The stereoscopic angles are defined as the angles of the triangle made up of the two intersecting lines of sight as well as the vector from one site to the other. Small stereoscopic angles sometimes happens when the sites are too close together, when a site is too close to the tracked object, or if the sensors are looking in nearly the same direction. Knowing the stereoscopic angles before running the algorithm allows a filter to be set to eliminate erroneous results and free up runtime.

$$\theta_1 = \text{acos}\left(\frac{(\vec{R}_2 - \vec{R}_1) * \hat{\rho}_1}{|\vec{R}_2 - \vec{R}_1|}\right) \tag{6}$$

$$\theta_2 = \text{acos}\left(\frac{(\vec{R}_1 - \vec{R}_2) * \hat{\rho}_2}{|\vec{R}_1 - \vec{R}_2|}\right) \tag{7}$$

$$\theta_3 = \text{acos}(\hat{\rho}_1 * \hat{\rho}_2) \tag{8}$$

Appendix B: Smoothing Algorithm [2, 4]

The smoothing algorithm utilizes a least-squares polynomial regression fit. If there is a series of measurements, *Y*, as a function of time, *T*, there exists a polynomial that best fits the data. It should be noted that due to measurement noise, a higher order polynomial may fit the data better but could give less accurate results when re-expanding the polynomial. Care should be taken not to use too high of an order in the fit or the fit will be too optimistic.

The best fit polynomial of order, *N*, has the form:

$$Y = a_N t^N + \cdots + a_2 t^2 + a_1 t + a_0 \tag{9}$$

In this case *Y* and *t* are known, so the coefficients of the polynomial, *a*, must be solved for. The first step is to find the average time of the track, $\bar{t}$, so that $t_i = T_i - \bar{t}$ for each measurement. Then the matrices can then be constructed.

The measurement matrix will have the form:

$$Y = \begin{bmatrix} Y_1 \\ \vdots \\ Y_m \end{bmatrix} \tag{10}$$

Where *m* is the number of measurements. *Y* can be any measurement to be fitted such as right ascension, declination, or range.

$$V = \begin{bmatrix} t_1^N & \cdots & t_1^0 \\ \vdots & \ddots & \vdots \\ t_m^N & \cdots & t_m^0 \end{bmatrix} \tag{11}$$

Once these two matrices are set up, they are put in the familiar least-squares form:

$$Va = Y \tag{12}$$

For an N^{th} order fit, *a* will take the form:

$$a = \begin{bmatrix} a_N \\ \vdots \\ a_1 \\ a_0 \end{bmatrix} \tag{13}$$

To solve the least-squares equation for *a*, a modified Householder orthogonal transformation is used [1]. The advantage of this algorithm is that the matrix doesn't have to be squared to be inverted. This allows the numerical precision to be better maintained. As an added bonus, the covariance and Root Mean Square (RMS) error of the fit are computed as well. If the RMS is too high, the order of the polynomial can be increased and the process repeated. This also keeps the order from going too high as it does in a Lagrange or Hermite polynomial interpolator.

Using the fit polynomial, a corresponding measurement, *Y*(*T*), and its derivatives can be interpolated for any time, *T*. This allows the user to time align observations from different tracks.